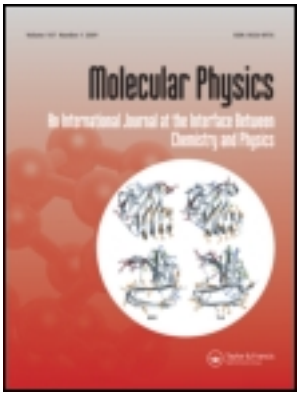

Molecular Physics: An International Journal at the Interface Between Chemistry and Physics

Publication details, including instructions for authors and subscription information:
http://www.tandfonline.com/loi/tmph20

Multiple-quantum N.M.R. study of molecular structure and ordering in a liquid crystal

S.W. Sinton [a b], D.B. Zax [a], J.B. Murdoch [a] & A. Pines [a]

[a] Department of Chemistry and Materials and Molecular Research Division, Lawrence Berkeley Laboratory, University of California, Berkeley, California, 94720, U.S.A.

[b] Exxon Production Research Company, P.O. Box 2189, Houston, Texas, 77001, U.S.A.

Version of record first published: 22 Aug 2006.

To cite this article: S.W. Sinton , D.B. Zax , J.B. Murdoch & A. Pines (1984): Multiple-quantum N.M.R. study of molecular structure and ordering in a liquid crystal, Molecular Physics: An International Journal at the Interface Between Chemistry and Physics, 53:2, 333-362

To link to this article: http://dx.doi.org/10.1080/00268978400102351

MOLECULAR PHYSICS, 1984, VOL. 53, NO. 2, 333–362

Multiple-quantum N.M.R. study of molecular structure and ordering in a liquid crystal

by S. W. SINTON†, D. B. ZAX, J. B. MURDOCH and A. PINES
Department of Chemistry and Materials and Molecular Research Division,
Lawrence Berkeley Laboratory,
University of California, Berkeley, California 94720, U.S.A.

(*Received* 25 *October* 1983 ; *accepted* 5 *May* 1984)

Proton multiple-quantum N.M.R. spectroscopy was used to investigate the anisotropic ordering in a magnetic field and molecular structure for the nematic phase of 4-cyano-4′-n-pentyl-d_{11}-biphenyl (5CB-d_{11}). The multiple-quantum spectra exhibit a greater resolution of line splittings than the conventional single-quantum Fourier transform N.M.R. spectrum of 5CB-d_{11}. This greatly simplifies a spectral analysis for the proton dipole–dipole coupling constants. Splittings among the five-, six-, and seven-quantum spectra are used to obtain the biphenyl proton couplings for 5CB-d_{11}. Two models for the biphenyl symmetry are considered in the analysis. In one model (D_4 symmetry), the two phenyl rings are assumed to be equivalent. In the other model (D_2 symmetry), the rings are inequivalent by virtue of structural or motional differences between them. Both models produce acceptable fits to the splittings assigned from the experimental spectra. However, we conclude that the spectra cannot be used to make a choice between D_2 and D_4 symmetry for the biphenyl group of 5CB-d_{11}. The proton dipolar couplings obtained in both cases are used to derive values for internuclear distances and the biphenyl order parameters. The D_4 symmetry dipolar couplings produce the most reasonable structural description of the biphenyl unit in which the phenyl ring geometry is close to that of benzene. The angle of twist between the ring planes is determined to be $30 \pm 2°$. The order parameters from the D_4 symmetry analysis are in good agreement with results reported by others for the same liquid crystal but with a higher degree of deuterium substitution. Possible causes for experimentally observed seven-quantum splittings that are not predicted by the symmetry model are discussed.

1. INTRODUCTION

The liquid crystalline phases of 4-cyano-4′-n-alkylbiphenyls have been studied by a number of techniques including X-ray [1], deuterium [2–4] and proton [5–7] N.M.R., infrared spectroscopy [8], and dielectric relaxation [9]. In this paper we report on our work with the five-carbon alkyl chain member of this series, 4-cyano-4′-n-pentylbiphenyl (abbreviated 5CB), in its nematic phase. We synthesized the deuterated analogue, 5CB-d_{11}, shown in figure 1, and used proton N.M.R. to investigate the average orientation and structure of the biphenyl moiety.

† Current address : Exxon Production Research Company, P.O. Box 2189, Houston, Texas 77001, U.S.A.

The nematic phase of 5CB is a uniaxial liquid crystal which is oriented when placed in a strong magnetic field. The nuclear spin hamiltonian for an oriented phase contains anisotropic interactions which cannot be determined in a liquid phase because of rapid, isotropic molecular motion. Previous studies of alkyl-cyanobiphenyl liquid crystals used deuterium N.M.R. and focused primarily on the anisotropic ordering of the alkyl chains. The strongest anisotropic interaction for deuterium nuclei is usually the quadrupolar coupling to local electric field gradients. Deuterium dipolar couplings are much weaker and often do not lead to resolved splittings in a deuterium spectrum of a liquid crystal.

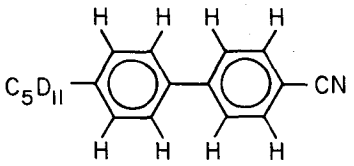

Figure 1. The molecule 4-cyano-4′-n-pentyl-d_{11}-biphenyl (5CB-d_{11}). In this work, proton multiple-quantum N.M.R. spectra are used to determine nematic phase order parameters and the structure of the biphenyl group of 5CB-d_{11}. A simple model is used for the biphenyl symmetry in the analysis.

Proton dipolar couplings are stronger than the corresponding deuterium couplings. Dipolar couplings have even been measured for protons separated by three or more angstroms. Since protons are spin-1/2 nuclei with no quadrupolar coupling, proton N.M.R. spectra of liquid crystals are dominated by splittings arising from homonuclear dipolar couplings. If coupling constants can be derived by an analysis of the spectrum, valuable information concerning molecular structure and the average molecular orientation becomes available.

From the large number of interacting protons in a liquid crystal, one might expect a spectrum with many overlapping lines. If the overall resolution is poor, an analysis for dipolar couplings may prove difficult. For 5CB-d_{11}, the eight aromatic protons give rise to more than 1000 N.M.R. transitions and individual lines in a conventional spectrum are poorly resolved. We have used a multiple-quantum N.M.R. experiment to simplify this situation by producing a tractable set of spectral parameters for analysis. This experiment, and a preliminary analysis of the multiple quantum spectrum, were reported in an earlier paper [6]. In this article we present a more thorough spectral analysis for proton dipolar couplings and a further analysis of these couplings in terms of internuclear distances and the average orientation of the biphenyl unit. We also discuss our results on a deuterium decoupled multiple-quantum experiment.

In the next section, we cover some background on multiple-quantum (MQ) N.M.R. of liquid crystals. In §§ 3 and 4 we describe the experiments and results on 5CB-d_{11}. In §§ 5 and 6 the dipolar couplings are derived and analysed for molecular parameters by considering simple models for the biphenyl symmetry. In § 6 we compare our results to those of Emsley *et al.* [4] on the same liquid crystal with a greater degree of isotopic substitution than 5CB-d_{11}. In § 7, possible sources of errors in the analysis of the MQ data are investigated.

2. Background theory

2.1. *Proton N.M.R. of liquid crystals*

Anisotropic interactions for an ensemble of nuclear spins can be expressed in terms of angular momentum operators and a second rank tensor describing each interaction. For proton spins in an oriented liquid crystal, the dipolar hamiltonian may be written

$$\mathscr{H}_D = \sum_{i<j} \mathbf{I}_i \mathbf{D}_{ij} \mathbf{I}_j, \tag{1}$$

where $\mathbf{D}_{ij}$ is the coupling tensor (in its principal axis system). The summation in equation (1) is restricted to intramolecular couplings. Intermolecular couplings are vanishingly small because of rapid diffusion. $\mathbf{I}_i$ is the spin angular momentum operator for nucleus i.

When a strong magnetic field is used, an N.M.R. experiment measures the secular component of $\mathscr{H}_D$ in a laboratory frame. Thus, a single value for the coupling of a pair of nuclei is available from the spectrum for any particular orientation of the liquid crystal director relative to this laboratory frame. Throughout this paper, we assume the liquid crystal is uniaxial with the director parallel to the field direction. Splittings in the spectrum arise from dipolar couplings which are averaged by the reorientational motions of liquid crystal molecules relative to the director.

Saupe introduced a second rank tensor which relates the laboratory frame value of a dipolar coupling measured from the spectrum to a molecule-fixed axis system by the cartesian product [10]

$$D_{ij} = \tfrac{2}{3} \sum_{\alpha\beta}^{x,y,z} \langle S_{\alpha\beta} (D_{\alpha\beta})_{ij} \rangle. \tag{2}$$

The elements of the traceless, symmetric tensor S are the order parameters given by

$$S_{\alpha\beta} = \tfrac{1}{2}(3\overline{l_\alpha l_\beta} - \delta_{\alpha\beta}), \tag{3}$$

where the l_α are direction cosines relating the molecule-fixed axis system to the magnetic field direction. The bar in equation (3) implies an average over the ensemble of molecular orientations relative to the director. Liquid crystal molecules are not completely rigid but rather consist of rigid sub-units capable of rotations relative to one another resulting in many possible molecular conformations. These internal motions most likely occur on a time scale ($\leqslant 10^{-9}$ s) much shorter than the inverse of the dipolar couplings (10^{-2} to 10^{-4} s). The D_{ij} are then values of couplings which are averaged by internal motions as implied by the angular brackets in equation (2) [11–13]. This average strictly should include vibrational motions as well as larger amplitude torsions or internal rotations. Transforming $\mathbf{D}_{ij}$ from its principal axis frame, we can rewrite equation (2) in terms of elements in the molecule-fixed frame as [14]

$$\begin{aligned} D_{ij} = -\frac{\gamma^2 h}{8\pi^2} \frac{1}{\langle r_{ij}^3 \rangle} \{ & \langle S_{zz}(3\cos^2\theta_{ijz} - 1) \rangle + \langle (S_{xx} - S_{yy})(\cos^2\theta_{ijx} - \cos^2\theta_{ijy}) \rangle \\ & + 4\langle S_{xy}(\cos\theta_{ijx}\cos\theta_{ijy}) \rangle + 4\langle S_{xz}(\cos\theta_{ijx}\cos\theta_{ijz}) \rangle \\ & + 4\langle S_{yz}(\cos\theta_{ijy}\cos\theta_{ijz}) \rangle \}, \end{aligned} \tag{4}$$

where γ is the proton gyromagnetic ratio. The angles θ_{ijp}, $p=x, y, z$, are between the internuclear vector r_{ij} and the x, y, z axes of the molecule-fixed frame.

The object of our analysis of the N.M.R. spectra is to derive the D_{ij} from transition frequencies and then extract values for the $S_{\alpha\beta}$ and r_{ij} using equation (4). This requires an understanding of how the internal motions affect both the nuclear coordinates and the $S_{\alpha\beta}$. In the general case, the potential field which determines the orientation of a molecule-fixed frame relative to the director is a function of the internal coordinates of the molecule [11–13]. Thus, the various conformations a molecule can adopt might each experience different orientational energies. This can complicate the interpretation of the coupling constants because each conformation must be described by its own order tensor and one usually does not know how the orientational potential varies with conformation.

When the magnetic interactions are confined to rigid sub-units of a non-rigid molecule, one can write an expression for the interactions in terms of a local order tensor for each sub-unit. Such is often the case for deuterium quadrupolar couplings obtained from N.M.R. spectra of deuterated liquid crystals (see for example, [3]). One is then left with the need to relate the local order tensors to one another in order to gain a knowledge of conformational probabilities. Alternatively, if conformational probabilities can be modelled, then the local order tensors and molecular geometry can be determined, provided there is enough information available from the spectra.

The proton dipolar interactions of 5CB-d_{11} present a somewhat different problem. Inter-ring couplings, which are averaged by torsional motions of the biphenyl rings about their C_2 axes, can be used to determine the angle of twist, or dihedral angle, between the rings. The symmetry and motion of the rings greatly reduces the number of unique interactions which must be determined from the spectra. Within certain simplifying assumptions which we allude to in § 6, this symmetry also simplifies the conformational averaging in the calculations using equation (4). We reduce the number of unique $S_{\alpha\beta}$ to be determined from the D_{ij} by the proper choice of molecule-fixed axis system and by recognizing how the orientational energies and geometric coordinates change with internal rotation [13, 15].

Initial estimates for the D_{ij} were calculated from equation (4) and the model for motional averaging. The usual least-squares spectral fitting techniques were then used to refine the values of the coupling constants. This procedure relies on our ability to make reasonable assignments of the calculated transition frequencies to those observed [16]. The multiple-quantum spectra contain enough well resolved lines for straightforward assignments to the calculated spectra. Finally, order parameters and internuclear separations were obtained by another least-squares fit to the D_{ij} using equation (4).

2.2. *Multiple-quantum N.M.R.*

Neglecting any non-linear response of a spin system to radio-frequency irradiation, conventional (or single-quantum) N.M.R. spectroscopy obeys the well-known selection rule $\Delta M=(M_i-M_j)=\pm 1$ where M_i and M_j are the total Zeeman quantum numbers for eigenstates i and j respectively. In an MQ experiment, this restriction is removed and lines corresponding to all possible values of ΔM ($\pm 2I$, $\pm(2I-1)$, . . . 0, with I the total spin) may be observed [17–19].

Greater resolution is expected for sets of lines corresponding to the highest values of ΔM (the ' high-order ' MQ subspectra) than for the single-quantum spectrum because fewer lines occur in the same spectral width [20, 21]. This increase in resolution is not necessarily accompanied by any loss of information about the dipolar couplings [22]. In fact, for the six- and seven-quantum orders of 5CB-d_{11}, it can be shown that splittings are quite sensitive to order parameters and the biphenyl structure [15]. In addition, molecular symmetry is often reflected in high-order spectra in a simple and predictable manner [22]. A full description of multiple-quantum N.M.R. theory is beyond the scope of this paper. The interested reader is directed to the excellent reviews by Weitekamp [23] and Bodenhausen [24].

3. Experimental

3.1. *Liquid crystal synthesis*

The synthesis of 5CB-d_{11} followed the procedure of Gray and Mosley [25] with a slight modification reported in our earlier paper [6]. About 400 mg of 5CB-d_{11} was sealed under vacuum in a six mm o.d. glass tube. This sample was used for all experiments described below.

3.2. *Spectrometers*

All spectra were collected on either of two home-built Fourier transform pulse spectrometers described elsewhere [15, 26]. These spectrometers are operationally identical except for a slight difference in field strength. The proton frequency for one is 182 MHz while for the other it is 185 MHz. With both instruments, the temperature in the sample region is maintained by a heated gas flow (air or N_2). Temperature in this flow is detected by a copper-constantan thermocouple placed near the sample (within approx. 1 cm) but outside the N.M.R. coil. Temperature determined by this thermocouple is regulated to within $\pm 0{\cdot}1$°C by a feedback circuit to the gas heater. For deuterium decoupling experiments in which coil heating was a problem, a large coil was used with the sample suspended in the centre of the coil by Teflon standoffs.

3.3. *Proton single-quantum spectrum*

The proton single-quantum spectrum was obtained by the standard single pulse, Fourier transform method. Deuterium decoupling was achieved by irradiation in the centre of the alkyl chain deuteron spectrum during the acquisition period. It has been demonstrated that deuterium double-quantum transitions are excited by this technique, increasing the decoupling efficiency over that of conventional broadband decoupling [27].

3.4. *Proton multiple-quantum spectra*

The proton MQ spectra were obtained with the pulse sequence shown in figure 2. The theory of MQ spectroscopy with this pulse sequence is given elsewhere [20]. We only point out its general features here. MQ coherences are ' prepared ' from the equilibrium spin system by the first two $\pi/2$ pulses. The delay of τ seconds between these pulses is necessary for efficient production of MQ coherences. The choice of τ is dictated by the size of the dipolar

couplings [28]. In practice, several values of τ are chosen and the resulting magnitude spectra are averaged together. In this way, MQ lines of low intensity for one choice of τ will still appear in the averaged spectrum provided a higher intensity is produced by some other value of τ.

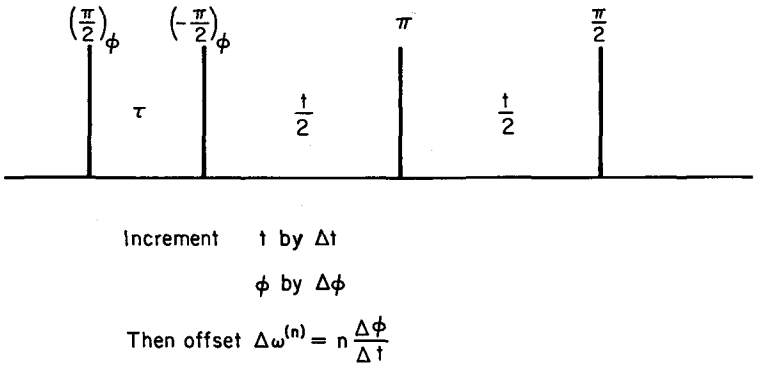

Figure 2. Radio frequency pulse sequence used to acquire the multiple-quantum N.M.R. spectra discussed in this paper. The carrier frequency for all pulses was placed at the centre of the proton single-quantum spectrum (figure 3). The π pulse served to remove line broadening caused by an inhomogeneous magnetic field. The magnetization was sampled τ seconds after the final $\pi/2$ pulse for a single set of values for t and ϕ, the phase of the first two pulses. Incrementing ϕ for each new value of t according to the prescription given in the figure leads to a frequency offset $\Delta\omega^{(n)}$ for each order n in the spectrum.

Once prepared, MQ coherences are allowed to evolve for a time t. Inhomogeneous broadening from magnetic field gradients is eliminated by a π pulse in the centre of this time period. This pulse causes a spin echo to form at the end of the evolution period [20]. Because chemical shifts and heteronuclear couplings are present in 5CB-d_{11}, complications can potentially arise from the use of this π pulse. This issue is taken up in detail in § 7.

Detection of a signal related to the evolution of MQ coherence is accomplished by applying a final $\pi/2$ ' mixing ' pulse. After another delay of τ seconds, the magnetization is sampled once. A multiple-quantum interferogram is collected by incrementing t in a series of acquisitions [6]. To avoid cancellation in the signal from different MQ orders, a modulation of the interferogram is produced by incrementing the phase of the first two pulses for each new value of t. This time proportional phase incrementation technique and the resulting order-dependent offsets of MQ lines are fully discussed elsewhere [20, 29]. Fourier transformation of the MQ interferogram results in an MQ spectrum.

For each of the MQ spectra of this work, a total of six interferograms were collected, each one 16 k data points long. Values of τ were incremented by 0·2 ms for each new interferogram. The initial τ value was 0·4 ms for the undecoupled MQ spectrum. In the experiments including deuterium decoupling, the initial τ value was 0·2 ms. For both experiments, t was incremented by 1 μs and the phase of the preparation pulse by 22·5° for each point in an interferogram. Each interferogram was zero-filled to 32 k points before Fourier tranformation.

4. Results

4.1. *Single-quantum spectrum*

The proton single-quantum N.M.R. spectrum of 5CB-d_{11} is shown in figure 3. Temperature was regulated at 26·0°C. The separately measured inhomogeneous linewidth of H_2O was 0·05 ppm. Lack of resolution in this spectrum is partly due to inhomogeneous broadening but also reflects the overlap of homogeneous linewidths from many closely spaced lines. No attempt was made to analyse this spectrum for dipolar couplings. Nonetheless, this experiment was useful for estimating the power requirements for double-quantum decoupling.

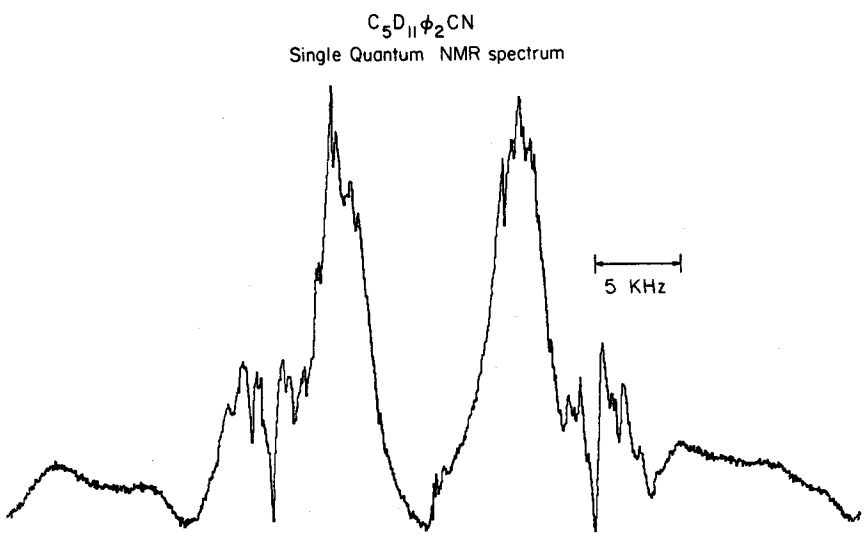

Figure 3. Proton single-quantum N.M.R. spectrum of 5CB-d_{11}. Deuterium decoupling was used to remove dipolar couplings between the protons and the alkyl deuterons. The total width shown is 50 kHz.

Pines *et al.* [27] have shown that efficient double-quantum decoupling of spin-1 nuclei is achieved by on-resonance irradiation when the magnitude of the radio frequency field, ν_1, in frequency units, is greater than that given by

$$\nu_1 \sim (\nu_Q \nu_D)^{1/2} \tag{5}$$

where ν_Q is the largest deuterium quadrupolar coupling and ν_D is the largest heteronuclear dipolar coupling. We found that no improvement in resolution for ν_1 greater than a few kHz. Emsley *et al.* [4] have measured the largest quadrupolar splitting for 5CB-d_{11}, assigned to the methylene group attached to the biphenyl ring, to be about 35 kHz at 26°C. From equation (5) then, ν_D must be on the order of 100 Hz.

4.2. *Proton MQ spectrum*

The proton MQ spectrum of 5CB-d_{11}, acquired without deuterium double-quantum decoupling and at a temperature of 26·0°C, is shown in figure 4. This spectrum consists of a progression of MQ orders from the zero-quantum

($\Delta M = 0$) up to the eight-quantum. One-half of the full MQ spectral width is shown in figure 4. A decrease in the number of lines with increasing ΔM is evident. Linewidths vary from 150 to 210 Hz.

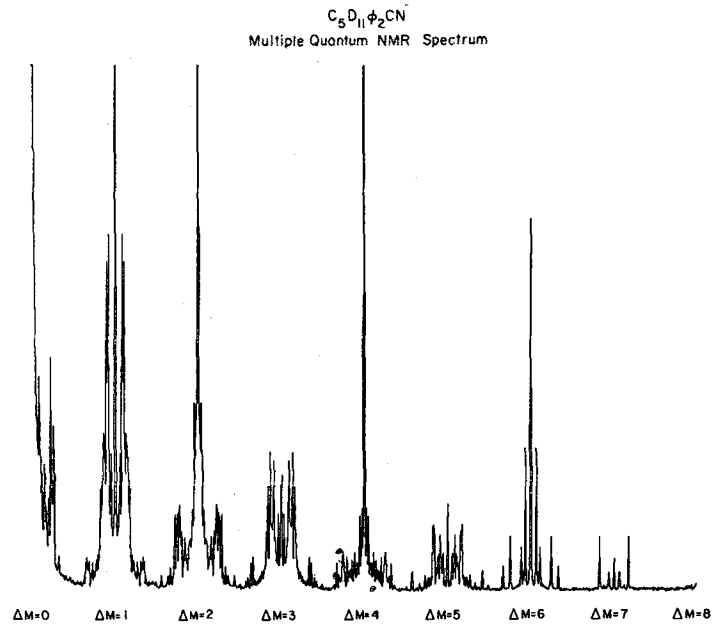

Figure 4. Proton multiple-quantum N.M.R. spectrum of 5CB-d_{11}. The individual multiple-quantum orders were separated by time proportional phase incrementation of r.f. pulses. The change in magnetic quantum number for each order, ΔM, is indicated beneath the corresponding subspectrum. Only one half of the symmetric zero and eight quantum regions are shown. The full width displayed is 500 kHz.

4.3. *Deuterium decoupled proton MQ spectrum*

The π pulse in the centre of the pulse sequence of figure 2 refocuses dephasing of MQ coherences caused by magnetic field gradients [20]. Modulations of MQ evolution caused by heteronuclear couplings are also partially refocused by this pulse. It has been argued [7, 30] that, in some cases, heteronuclear couplings are sufficiently cancelled by a single refocusing π pulse to effectively decouple heteronuclear spins. In an effort to determine the extent of any distortions of the MQ spectrum caused by incomplete refocusing of proton–deuterium dipolar couplings, we proceeded with a second experiment in which deuterium decoupling irradiation was used. Conditions for decoupling were determined in the decoupled single-quantum experiment (figure 3). The resulting MQ spectrum is shown in figure 5.

There is a significant decrease in the signal-to-noise ratio for the spectrum of figure 5 compared to that in figure 4. There are several possible causes of this loss of S/N. A smaller filling factor for the larger coil volume used in the decoupling experiment leads to a decrease in signal. Temperature gradients in the sample may also have been a problem. As evidence for this we note that individual lines with large splittings from the centre of an order are somewhat broader than those close to the centre. One possible source of added noise in

the decoupled experiment may have been fluctuations in the prepared MQ coherences caused by instrumental instabilities [23]. None the less, the decoupling did evidently remove some residual dipolar broadening from the MQ spectrum; some lines in figure 5 are slightly narrower (120 Hz) than their counterparts in figure 4. A comparison is not quantitative, however, because the temperature in the decoupled experiment (28·9°C) was somewhat higher.

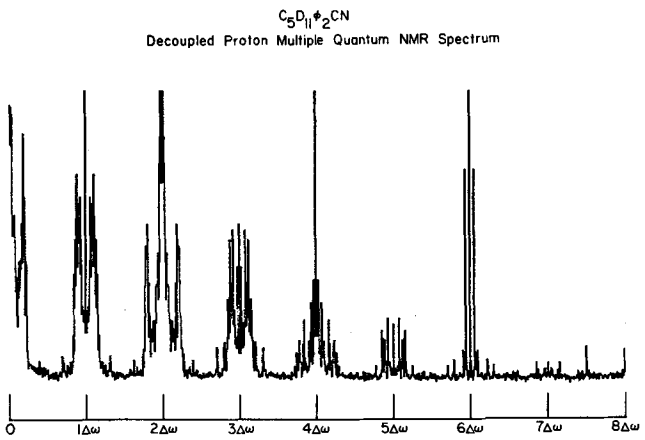

Figure 5. Deuterium decoupled proton multiple-quantum N.M.R. spectrum of 5CB-d_{11} at 28·9°C. The experimental conditions were similar to those used to obtain the undecoupled spectrum of figure 4. A deuterium decoupling pulse was applied for the duration of the pulse sequence in figure 2 for each point in the multiple-quantum interferogram. The total width shown is 500 kHz.

5. Analysis of the proton MQ spectra for dipolar coupling constants

We can considerably simplify the analysis of the spectra in figures 4 and 5 by considering the symmetry of the biphenyl unit. We proceed by making a few assumptions about the torsional motion of the two rings.

5.1. *Biphenyl conformations*

The phenyl rings of a biphenyl group are capable of rotating about an axis defined by their inter-ring bond. The angular displacement between the ring planes is characterized by a dihedral angle ϕ. The effects of torsional motions about ϕ on the dipolar coupling constants of an oriented biphenyl have already been treated in several papers [31–33]. We review here the important points necessary for our analysis.

We first assume that the torsional motion is fast compared to the inverse of couplings which depend on ϕ. Proton N.M.R. spectra of substituted biphenyls dissolved in liquid crystals have been found to be inconsistent with slow ring torsions [31–33]. The potential energy for the motion is then assumed to be symmetric such that four equivalent conformations exist for each value of ϕ, as depicted in figure 6. The minima in the potential occur at the dihedral angles $\pm\phi_m$ and $\pi \pm \phi_m$. Unhindered rotation of the rings was ruled out because the motionally averaged couplings would be reduced in magnitude considerably from what we find in our analysis [15].

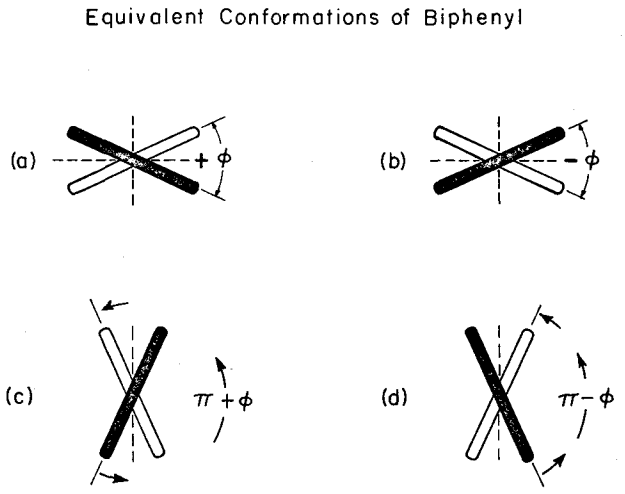

Figure 6. Four equivalent conformations of a biphenyl group for dihedral angles $\pm\phi$ and $\pi \pm \phi$. In each drawing ((*a*)–(*d*)), the biphenyl group is viewed along its major C_2 axis with the ring planes perpendicular to the plane of the figure. The phenyl rings are represented by the filled and open rectangles. Rapid exchange between these four conformations is assumed in the analyses described in the text. This motion creates two effective mirror planes containing the dotted lines.

5.2. *Biphenyl symmetry models*

Before going on with an analysis of the spectra, we can get some idea of what to expect by considering some simple symmetry arguments. From a symmetry analysis, we can calculate the maximum number of lines possible in each multiple-quantum order and compare these numbers to the spectra in figures 4 and 5. This is a useful exercise for multiple-quantum spectra of symmetric molecules because the high order subspectra often consist of only a few lines for comparison [22].

We begin by considering the symmetry of a 4,4′-disubstituted biphenyl. The permutation symmetry for the protons of each ring is isomorphous with the C_2 point group. There are then two possibilities for the permutation symmetry for all the protons of the biphenyl group. Either the two rings are equivalent or they are not. The rings must be considered inequivalent if there are structural differences or, even for structurally identical rings, if there are motional differences between them. Motional inequivalencies would arise if one ring is more hindered in its rotation or reorientation than the other. Inequivalent reorientational motions lead to different local order matrices for the two rings.

For the case of inequivalent phenyl rings, the full permutation group for the protons of a 4,4′-substituted biphenyl is isomorphous with the D_2 point group. If the rings are actually equivalent, then there must exist a symmetry element which exchanges them, and the permutation group is D_4. A D_2 symmetry 4,4′-substituted biphenyl has a total of 12 unique couplings ; four within each ring and four inter-ring couplings which are sensitive to the dihedral angle and off-diagonal elements of the order tensor (see below). The number of intra-ring

couplings are identical for D_4 symmetry and there are only three unique inter-ring couplings. The permutation group for the protons of 5CB-d_{11} is D_2 because of inequivalent substituents (alkyl and cyano). However, if the ring structures do not deviate significantly and their local order matrices are nearly equal, then a proton N.M.R. spectrum will reflect an effective D_4 symmetry. One object of our analysis was to determine if multiple-quantum spectra can distinguish between D_2 and D_4 symmetry for the biphenyl protons of 5CB-d_{11}.

5.3. *Energy level diagrams and predicted numbers of MQ lines*

Using standard group theory and the properties of the D_2 and D_4 point groups, we can straightforwardly predict the distribution of eigenstates among the irreducible representations. Figures 7 and 8 show the symmetrized energy level diagrams for protons in a D_4 or D_2 permutation group, respectively. The familiar restriction of N.M.R. transitions to eigenstates of the same irreducible representation [34] (neglecting any symmetry-breaking relaxation effects) allows us to predict the number of lines possible for each MQ order. These numbers are given for D_4 symmetry in table 1 and D_2 in table 2. The number of MQ lines in the seven- and six-quantum orders can also be predicted by considering the number of unique spins which are allowed by the symmetry elements of the point group [22].

Symmetrically Para-substituted Biphenyl

D_4 Point Group Energy Level Diagram

M	A_1	A_2	B_1	B_2	E
-4	1				
-3	2			2	2X2
-2	7	1	3	5	2X6
-1	10	4	4	10	2X14
0	15	5	7	11	2X16
1	10	4	4	10	2X14
2	7	1	3	5	2X6
3	2			2	2X2
4	1				

Figure 7. Energy level diagram for the eight proton spins of a symmetrically para-substituted biphenyl (D_4 symmetry). The six irreducible representations are indicated at the top. The E representation is doubly degenerate. Values for the total Zeeman quantum number M are shown along the left hand side. Numbers beneath each irreducible representation symbol are the dimensions of the Zeeman submatrices within that representation.

Asymmetrically Para-substituted Biphenyl

D_2 Point Group Energy Level Diagram

M	A_1	B_1	B_2	B_3
-4	1			
-3	4		2	2
-2	12	4	6	6
-1	20	8	14	14
0	26	12	16	16
1	20	8	14	14
2	12	4	6	6
3	4		2	2
4	1			

Figure 8. Energy level diagram for the eight proton spins of an asymmetrically para-substituted biphenyl (D_2 symmetry). The four irreducible representations are indicated at the top. Values of the total Zeeman quantum number are along the left hand side. Numbers given for each representation are the dimensions of the Zeeman submatrices for that represention.

Table 1. Predicted number of lines in the multiple-quantum spectrum of D_4 symmetry para-substituted biphenyl.

n-Quantum order	Lines†	Representation
8	1	A_1
7	4 (2 doublets)	A_1
6	14 (7 doublets)	A_1
	4 (1 : 2 : 1 triplet)	A_1
	4 (1 : 2 : 1 triplet)	B_2
	2 × 4 (1 : 2 : 1 triplet)	E
	21 total non-degenerate frequencies	
5	68 (34 doublets)	A_1
	20 (10 doublets)	B_2
	2 × 24 (12 doublets)	E
	112 total non-degenerate frequencies	
4	286 total	
3	628 total	
2	1142 total	
1	1580 total	

† For 8, 7, 6 and 5-quantum, a breakdown by representation is given with the total number of non-degenerate frequencies listed (ignoring accidental degeneracies). The doubly degenerate E representation is counted only once in the totals.

Table 2. Predicted number of lines in the multiple-quantum spectrum of a D_2 symmetry para-substituted biphenyl.

n-Quantum order	Lines†	Representation
8	1.	A_1
7	8 (4 doublets)	A_1
6	24 (12 doublets)	A_1
	24 (6 1 : 2 : 1 triplets)	A_1
	4 (1 : 2 : 1 triplet)	B_2
	4 (1 : 2 : 1 triplet)	B_3
	41 total non-degenerate frequencies	
5	136 (68 doublets)	A_1
	24 (12 doublets)	B_2
	24 (12 doublets)	B_3
	184 total non-degenerate frequencies	
4	556 total	
3	1256 total	
2	2256 total	
1	3160 total	

† For 8, 7, 6 and 5-quantum, a breakdown by representation is given. Only non-degenerate frequencies are counted in totals (ignoring accidental degeneracies).

5.4. *Dipolar couplings using D_4 symmetry model*

A computer program was written to simulate MQ spectra using values for D_{ij} and J_{ij} as input. In this program, the hamiltonian matrix is constructed from the D_{ij} and J_{ij} and from simple product basis functions. Permutation symmetry is imposed on the hamiltonian by setting couplings related by symmetry elements equal. After diagonalization of the hamiltonian, eigenvectors are sorted by symmetry representation on the basis of their matrix elements with I_x. Allowed multiple-quantum frequencies are chosen by examination of the symmetrized energy level diagram.

This computer program neglects chemical shifts and heteronuclear couplings. These spin interactions are at least partially removed from MQ evolution by the spin–echo refocusing action of the π pulse in figure 2. Possible errors caused by neglect of shifts and heteronuclear couplings are addressed in the last section. The most resolved portions of the multiple-quantum spectra are the five-, six-, and seven-quantum orders and assignments of lines in these orders to the computer simulated spectra were easily made. Least-squares reduction of the rms fit of these assignments was then used to refine the dipolar coupling constants. These calculations were performed in a manner similar to the LAOCOON least-squares spectral fitting routine [35] but modified specifically for MQ spectra [15].

In our original analysis [6], a total of 24 lines from among the five-, six-, and seven-quantum orders were assigned and the seven couplings unique for D_4 symmetry varied in the iteration. The resulting dipolar couplings are reproduced in table 3. The final rms deviation of splittings for calculated lines

from their assigned experimental counterparts is 26 Hz, below the digital resolution of the spectrum (30 Hz). The numbering of protons used for the couplings in table 3 follows figure 9. The two coordinate systems in figure 9 are explained below.

Table 3. Experimental proton coupling constants for 5CB-d_{11} assuming D_4 symmetry†.

Dipolar coupling constants/(Hz)‡		Scalar coupling constants/(Hz)§	
	Intra-ring (A and B)		
$D_{12}=D_{56}$	-4478 ± 2	$J_{12}=J_{56}$	8·0
$D_{14}=D_{58}$	380 ± 3	$J_{14}=J_{58}$	2·0
$D_{23}=D_{67}$	390 ± 3	$J_{23}=J_{67}$	2·0
$D_{13}=D_{57}$	47 ± 2	$J_{13}=J_{57}$	0·0
	Inter-ring		
D_{15}	-147 ± 2	J_{15}	0·0
$D_{16}=D_{25}$	-365 ± 2	$J_{16}=J_{25}$	0·0
D_{26}	-1741 ± 3	J_{26}	0·0

† From an iterative fit to the spectrum of figure 4. Numbering according to figure 9.
‡ Errors estimated from the rms error of the iterative fit.
§ Assumed values.

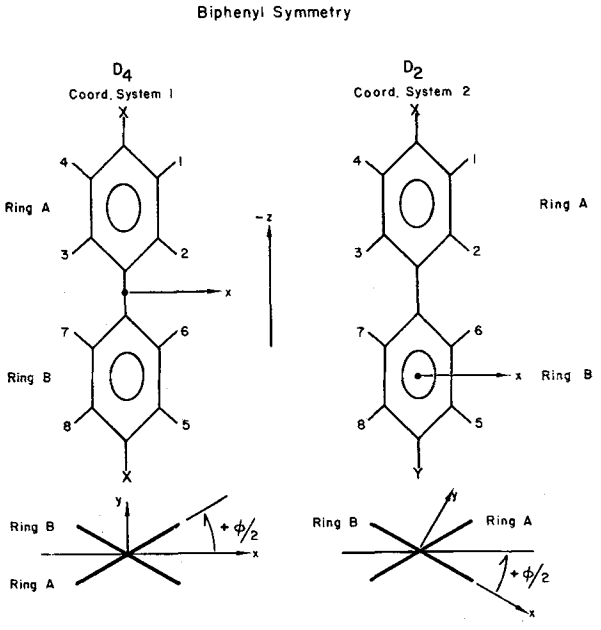

Figure 9. Coordinate systems and numbering of protons used to analyse the proton multiple-quantum spectra of 5CB-d_{11}. Coordinate system 1 for the D_4 symmetry case (left hand side) has its origin at the centre of the inter-ring carbon–carbon bond. The x and y axes then bisect the inter-ring dihedral angles. Coordinate system 2 for the D_2 symmetry case (right hand side) is attached to ring B with the x axis in the ring plane. Projections defining the direction of positive ϕ (bottom) are obtained by viewing down the z axis onto the xy plane.

Table 4. Experimental proton coupling constants for 5CB-d_{11} assuming D_2 symmetry†.

Dipolar coupling constants/(Hz)‡		Scalar coupling constants/(Hz)§	
	Ring *A*		
D_{12}	-4460 ± 3	J_{12}	8·0
D_{14}	463 ± 5	J_{14}	2·0
D_{23}	291 ± 7	J_{23}	2·0
D_{13}	72 ± 4	J_{13}	0·0
	Ring *B*		
D_{56}	-4500 ± 2	J_{56}	8·0
D_{58}	318 ± 5	J_{58}	2·0
D_{67}	458 ± 5	J_{67}	2·0
D_{57}	70 ± 2	J_{57}	0·0
	Inter-ring		
D_{15}	-150 ± 2	J_{15}	0·0
D_{16}	-409 ± 3	J_{16}	0·0
D_{25}	-360 ± 3	J_{25}	0·0
D_{26}	-1721 ± 2	J_{26}	0·0

† From an iterative fit to the spectrum of figure 4. Numbering according to figure 9.
‡ Errors estimated from the rms error of the iterative fit.
§ Assumed values.

5.5. *Dipolar couplings using D_2 symmetry model*

Close examination of the spectrum in figure 4 indicates that the two lines of the inner pair in the seven-quantum order are actually split. This conflicts with the predictions for D_4 symmetry (table 1). In addition, several lines in the five- and six-quantum orders have no close match to lines in the simulated spectrum. Because D_2 symmetry results in a greater number of lines for these orders, we proceeded with a second analysis with this symmetry model. The same 24 line assignments used for the D_4 analysis were again used to refine the 12 unique D_2 couplings. The results are given in table 4. The final rms error for this fit is only slightly smaller than for the D_4 symmetry fit (13·5 Hz). Several other line assignment possibilities were tried with no general improvement in the fit.

5.6. *Computer simulated spectra*

The MQ experiment was simulated using the pulse sequence of figure 2 and the refined dipolar coupling constants of tables 3 and 4. Intensities were calculated by using the same values for the preparation and detection delay τ as those actually used in the experiments. These ' exact τ averaged ' simulated spectra are shown for the five-, six-, and seven-quantum orders in figures 10 through 15. Figures 10–12 show the spectra calculated from values for D_4 couplings in table 3. Figures 13–15 show the comparison of calculated spectra using the D_2 couplings of table 4 and the experimental spectra. The effects of chemical shifts and heteronuclear couplings were not included in these calculations. Intensity distortions from the π pulse as a result of these interactions

could, in principle, be included in the calculations, given a knowledge of shifts and proton–deuterium coupling constants. Detailed descriptions of the computer programs used for these exact τ-averaged simulations are given elsewhere [36].

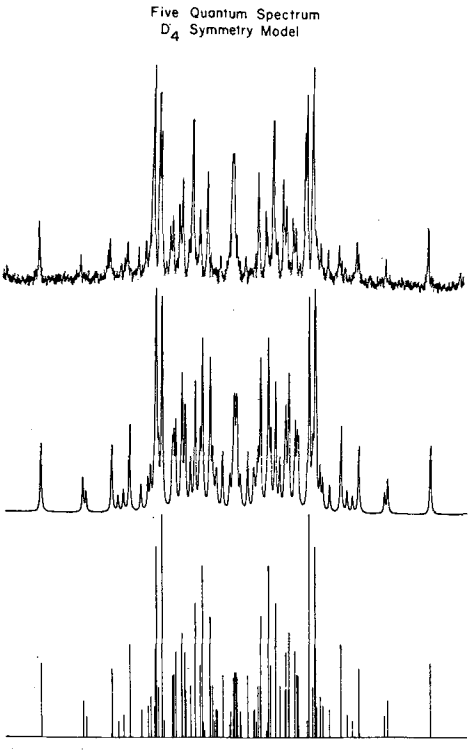

Figure 10. Five-quantum spectral fit assuming D_4 symmetry for the biphenyl group in 5CB-d_{11}. (*a*) Expanded trace of the five-quantum region of figure 4. Total frequency width shown is 62·5 kHz. (*b*) and (*c*) Theoretical spectra calculated from the couplings of table 3. Intensities are the result of exact calculations using the same values of the preparation time τ as chosen for the experiment. In (*b*) the theoretical spectrum has been broadened with a Lorentzian function to match the linewidths in (*a*).

The quality of the match between D_2 simulations and experimental spectra (figures 13–15) is similar to that for the D_4 spectra (figures 10–12). This indicates that the non-equivalence of the rings may not appreciably reduce the biphenyl symmetry from a perfect D_4 point group. Very few spectral features not already fit by the D_4 symmetry simulations are available for determining the larger number of independent couplings for the D_2 case. The error limits in tables 3 and 4 in fact reflect a poorer determination of the 12 coupling parameters in the D_2 fit than the seven D_4 parameters. The rms error for the D_4 symmetry

fit is already below the digital spectral resolution and so no significant improvement can be expected for these line assignments by using a different model for the proton spin symmetry. Thus, we conclude that the multiple-quantum spectrum of figure 4 cannot be used to distinguish between D_2 and D_4 proton symmetry for 5CB-d_{11} based on the line assignments chosen.

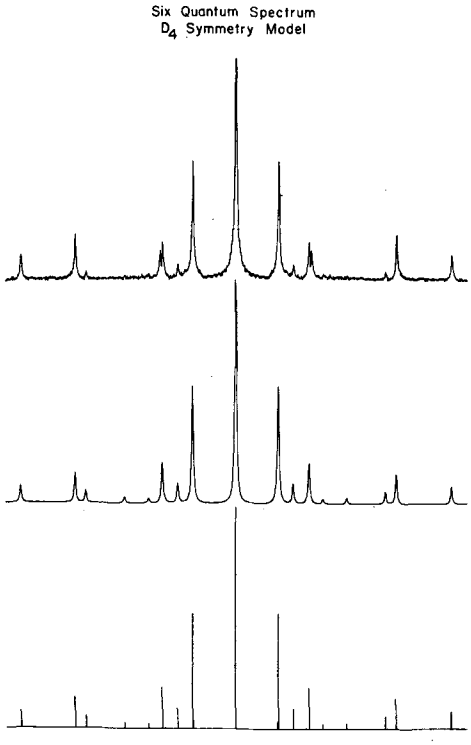

Figure 11. Six-quantum spectral fit assuming D_4 symmetry for the biphenyl group in 5CB-d_{11}. (*a*) Expanded trace from figure 4. Total width shown is 44189 Hz. (*b*) and (*c*) Theoretical spectra calculated from the couplings of table 3 and values of τ used in the experiment. Line broadening in (*b*) is intended to match the linewidths in (*a*).

5.7. *Analysis of decoupled MQ spectra for dipolar coupling constants*

The deuterium double-quantum decoupled MQ spectrum of figure 5 was analysed for dipolar couplings assuming D_4 symmetry. As a result of the poor S/N of the high order subspectra, only 13 lines could be assigned among the five-, six-, and seven-quantum regions of figure 5. The final rms error of the fit is 21·2 Hz. The refined couplings are given in table 5. Attempts to determine 12 independent D_2 symmetry couplings from these line assignments failed to converge to a close fit. Although it was not attempted in this work, a better fit might possibly be obtained by using resolved lines in the lower order regions of this spectrum.

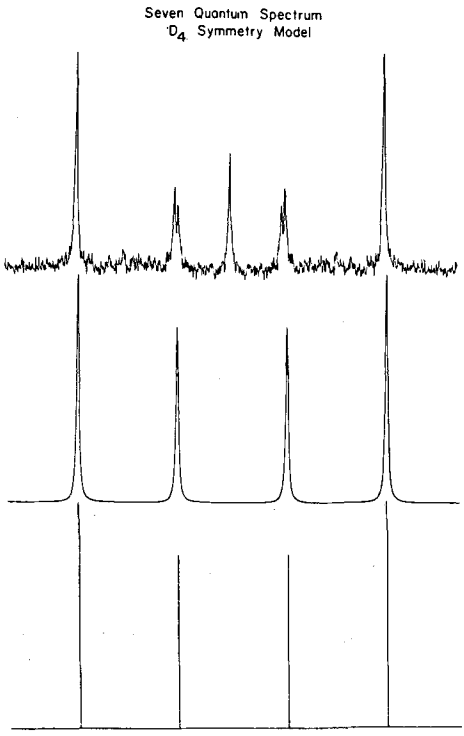

Figure 12. Seven-quantum spectra fit assuming D_4 symmetry for the protons of 5CB-d_{11}. (*a*) Expanded trace of the seven-quantum region of figure 4. Total width shown is 31982 Hz. The central line is most likely the result of pulse imperfections and multiple-quantum coherence transfer modulations caused by heteronuclear dipolar couplings (see text). (*b*) and (*c*) Theoretical spectra calculated from the couplings of table 3. The Lorentzian broadening in (*b*) matches the outer transitions in (*a*).

6. Analysis of dipolar couplings for order parameters and biphenyl structure of 5CB-d_{11}

6.1. *Simplifications for biphenyl symmetry*

From equation (4), we can use the dipolar couplings to determine order parameters and internuclear separations for 5CB-d_{11}. A complete treatment would require averaging over reorientations of the molecule, torsional motions of the rings, and vibrational displacements of the protons. Vibrational corrections to calculated D_{ij}s are usually small and in what follows have been neglected. The torsional motion of the rings could be handled by averaging with a potential parameterized by the barrier heights [31–33]. We adopt a simpler approach in which the torsions are averaged from the minimum energy conformations only. There are four such conformations characterized by periodic values of the dihedral angle (see figure 6) at the minima of the four-fold rotational potential $\pm\phi_m$, $\pi \pm \phi_m$.

Table 5. Proton coupling constants determined from the deuterium decoupled multiple-quantum N.M.R. spectrum of 5CB-d_{11} assuming D_4 symmetry.

Dipolar coupling constants/(Hz)†		Scalar coupling constants/(Hz)‡	
	Intra-ring (A and B)		
$D_{12}=D_{56}$	-3909 ± 4	$J_{12}=J_{56}$	8·0
$D_{14}=D_{58}$	289 ± 10	$J_{14}=J_{58}$	2·0
$D_{23}=D_{67}$	360 ± 6	$J_{23}=J_{67}$	2·0
$D_{13}=D_{57}$	44 ± 4	$J_{13}=J_{57}$	0·0
	Inter-ring		
D_{15}	-113 ± 5	J_{15}	0·0
$D_{16}=D_{25}$	-327 ± 3	$J_{16}=J_{25}$	0·0
D_{26}	-1529 ± 6	J_{26}	0·0

† Errors estimated from the rms error of an iterative fit to the spectrum in figure 5.
‡ Assumed values.

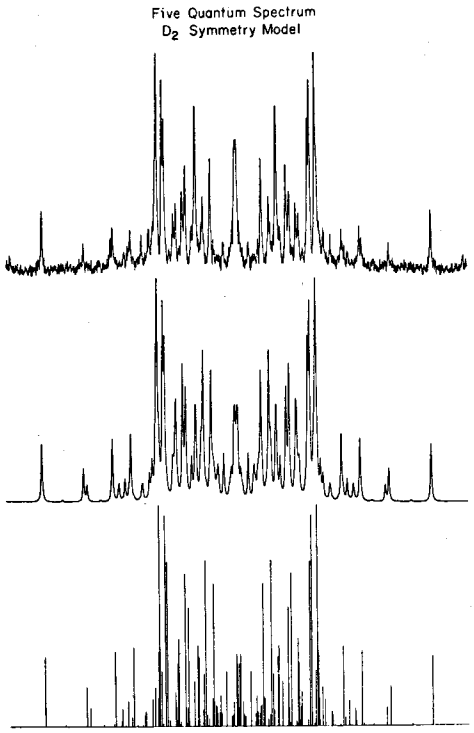

Figure 13. Five-quantum spectral fit assuming D_2 symmetry for the protons of 5CB-d_{11}. In (*a*) the experimental trace of figure 10 is repeated. The theoretical spectra in parts (*b*) and (*c*) were calculated from the couplings of table 4 and the values of τ used in the experiment.

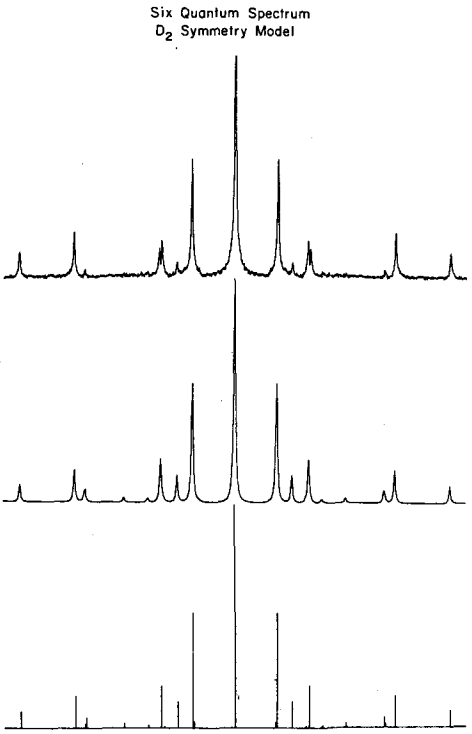

Figure 14. Six-quantum spectral fit assuming D_2 symmetry for the protons of 5CB-d_{11}. The coupling values of table 4 were used in the computer calculations. The spectra width shown is 44189 Hz.

The conformational averaging required in equation (4) is simplified by re-writing equation (2) for discrete conformations,

$$D_{ij} = \tfrac{2}{3} \sum_{\alpha\beta}^{x,y,z} \langle S_{\alpha\beta}{}^{n} (D_{ij})_{\alpha\beta}{}^{n} \rangle_{n,\,\mathrm{int}}, \tag{6}$$

where each conformation n enters into the average weighted by its probability. Similar to equation (4), the dipolar coupling between nuclei i and j for a single rigid conformation, averaged by reorientational motions, can be written as

$$\begin{aligned} D_{ij}{}^{n} = \frac{-\gamma^2 h}{8\pi^2} \frac{1}{(r_{ij}{}^{3})_n} \{ & S_{zz}{}^{n} (3\cos^2\theta_{ijz} - 1)_n \\ & + (S_{xx}{}^{n} - S_{yy}{}^{n})(\cos^2\theta_{ijx} - \cos^2\theta_{ijy})_n + 4S_{xy}{}^{n}(\cos\theta_{ijx}\cos\theta_{ijy})_n \\ & + 4S_{xz}{}^{n}(\cos\theta_{ijx}\cos\theta_{ijz})_n + 4S_{yz}{}^{n}(\cos\theta_{ijy}\cos\theta_{ijz})_n \}. \end{aligned} \tag{7}$$

To determine how many order parameters are required to define the 5CB-d_{11} couplings, we begin by considering conformations related by the dihedral angle, ϕ, (figure 6) and the same fixed conformation of the alkyl chain. The best choice for molecule-fixed axes is shown on the right hand side of figure 9

(coordinate system 2). This frame has its origin fixed in one of the rings (ring B) with the xy plane coplanar with this ring. Couplings within ring B depend on only $S_{zz}{}^n$ and $(S_{xx}{}^n - S_{yy}{}^n)$ since all r_{ij} lie in the xy plane. These order parameters are equal for each of the conformations of figure 6 and we henceforth drop the superscript n. Within ring A, D_{14} and D_{23} depend on S_{zz} and $(S_{xx} - S_{yy})$ and one off-diagonal element, $S_{xy}{}^n$. All other couplings (D_{12}, D_{13}, and inter-ring D_{ij}) depend on all five $S_{\alpha\beta}{}^n$. Because the conformations are related by reflection in the yz and xz planes, the following relationships among the off-diagonal elements can be established from equation (2) [4, 13, 15]:

$$S_{xy}{}^{\phi} = -S_{xy}{}^{-\phi} = S_{xy}{}^{\pi+\phi} = -S_{xy}{}^{\pi-\phi}, \tag{8 a}$$

$$S_{xz}{}^{\phi} = S_{xz}{}^{-\phi} = -S_{xz}{}^{\pi+\phi} = -S_{xz}{}^{\pi-\phi}, \tag{8 b}$$

$$S_{yz}{}^{\phi} = -S_{yz}{}^{-\phi} = -S_{yz}{}^{\pi+\phi} = S_{yz}{}^{\pi-\phi}. \tag{8 c}$$

The direction cosines of the r_{ij} also are related by sign changes for the four conformations. The result is that couplings within ring A, averaged over the four conformations, depend on only S_{zz}, $(S_{xx} - S_{yy})$ and S_{xy} while all five $S_{\alpha\beta}$ appear in the expressions for the averaged inter-ring couplings. The actual orientation of the liquid crystal molecules is described by an average over all conformations of the alkyl chain, each with its own order tensor. Proton

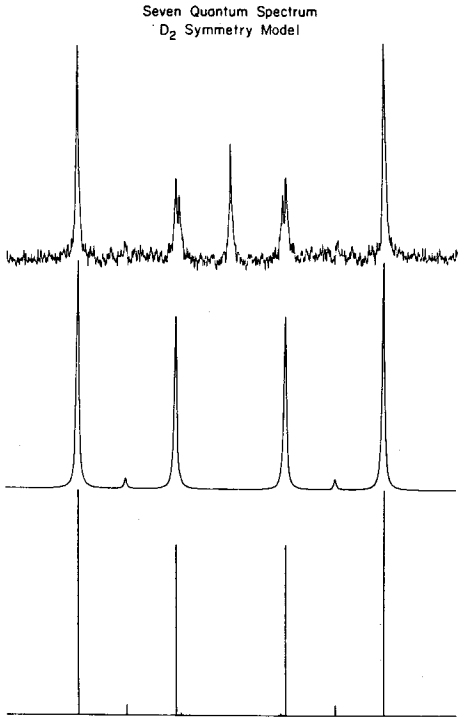

Figure 15. Seven-quantum spectral fit assuming D_2 symmetry for the protons of 5CB-d_{11}. Part (*a*) is the same as part (*a*) of figure 12. The couplings values of table 4 were used to calculate (*b*) and (*c*).

N.M.R. spectra of 5CB-d_{11} are sensitive only to dipolar couplings fully averaged over all chain conformations and obviously do not contain sufficient information to obtain the individual $S_{\alpha\beta}{}^n$ for each chain conformation. (Hereafter, all superscripts on the $S_{\alpha\beta}$ are dropped.)

With this model for the motional averaging of equation (4), a least-squares iterative fit was used to extract the order parameters and r_{ij}s from the D_{ij} values of tables 3, 4 and 5. This was accomplished with a computer program modelled after the program SHAPE [37]. We are indebted to Drs. Diehl and Bosiger for providing us with a copy of their program. The results are discussed in the following paragraphs. Errors for these parameters were propagated directly from the variance–covariance matrix for the D_{ij} parameters from the spectral fits. For all the least-squares iterations it was necessary to fix at least one parameter in order to achieve an adequate fit.

6.2. *Analysis of D_4 couplings*

If the structures and local order tensors for the two rings are so similar that the spectra indeed cannot distinguish between D_2 and D_4 symmetry, then the couplings obtained from the D_4 fit to figure 4 may provide an adequate description of the r_{ij}. In this case, the local ring order tensors should be related by a simple coordinate transformation. The most convenient coordinate system to then use is coordinate system 1 shown on the left hand side of figure 9. Coordinate system 1 is related to system 2 by a rotation of $\phi/2$ degrees about z and relocation of the origin to the mid-point of the ring–ring bond. In this frame, the order tensor is diagonal for D_4 symmetry. There are then seven parameters (three intra-ring distances, the inter-ring separation, ϕ_m, and two order parameters) to be determined from the couplings of table 3. The best fit was obtained by holding one of these parameters constant while varying the rest.

The D_4 couplings of table 3 yielded the molecular parameters of table 6 with an rms deviation of calculated to experimental couplings of 10·1 Hz. The final ring geometry is essentially the same as that of benzene ($r_{12}=r_{34}=r_{56}=r_{78}=$ 2·482 Å, $r_{14}=r_{23}=r_{58}=r_{67}=4{\cdot}299$ Å). The distance r_{260} in table 6 is the difference

Table 6. Internuclear distances, order parameters, and dihedral angle for 5CB-d_{11} determined with assumption of D_4 symmetry†.

r_{ij}/(Å)		$S_{\alpha\beta}$§	
r_{12}	2·47 ± 0·02	S_{zz}	0·565 ± 0·010
r_{14}	4·299‡	$(S_{xx}-S_{yy})$	0·071 ± 0·007
r_{23}	4·27 ± 0·03		
r_{260}‖	1·98 ± 0·03		
	ϕ_m/(degrees)		
	30·4 ± 2		

† From an iterative fit to the coupling constants of table 3. Errors estimated by method described in text. Numbering according to figure 9.

‡ Fixed at assumed value.

§ For coordinate system 1 of figure 9.

‖ r_{260} is the z-axis separation of protons 2 and 6.

in z-axis coordinates for protons 2 and 6. This distance has been measured for a variety of unsubstituted and substituted biphenyls in gas, solid and liquid crystal environments and is generally found to be close to 1·8 Å. The value determined from the D_4 couplings (1·98 Å) is thus larger than expected. This may arise from our neglect of vibrational averaging.

Emsley *et al.* [4] determined the local order parameters for the cyano-substituted ring of 5CB-d_{15} from measurements of the proton dipolar couplings. Their analysis assumed a ring geometry equivalent to that of benzene and included vibrational corrections for the D_{ij} based on a normal mode analysis for 4,4′-bipyridyl. A close correspondence exists between their order parameters determined at 26°C ($S_{zz} = 0{\cdot}565 \pm 0{\cdot}001$, $(S_{xx} - S_{yy}) = 0{\cdot}073 \pm 0{\cdot}006$) and those of table 3 (also at 26°C). The inclusion of vibrational averaging in our analysis would tend to increase our values for the order parameters and perhaps make this agreement less exact.

6.3. *Analysis of D_2 couplings*

For a D_2 symmetry analysis, a total 13 parameters must be determined for a full description of orientation and structure (three distances for each ring, the inter-ring separation, ϕ_m, and five order parameters). Only 12 couplings are available and so the value of at least one parameter must be assumed. In light of the fairly successful D_4 analysis described above, the off-diagonal order parameters may be quite small and we proceeded by neglecting S_{xz} and S_{yz}. This may indeed be a drastic assumption and we return to it in the next section.

Even with $S_{xz} = S_{yz} = 0$, we found that a successful iteration required holding one parameter constant. The results for two cases are given in table 7. The

Table 7. Internuclear distances, order parameters, and dihedral angle for 5CB-d_{11} determined with assumption of D_2 symmetry†.

	r_{ij}/(Å)	
	Case *A*	Case *B*
r_{12}	2·32 ± 0·05	2·453 ± 0·003
r_{14}	3·88 ± 0·09	4·11 ± 0·03
r_{23}	4·54 ± 0·09	4·81 ± 0·03
r_{56}	2·32 ± 0·04	2·456 ± 0·003
r_{58}	4·41 ± 0·17	4·67 ± 0·10
r_{67}	3·90 ± 0·13	4·14 ± 0·06
r_{260}	1·818†	1·93 ± 0·04
	$S_{\alpha\beta}$§	
S_{zz}	0·48 ± 0·03	0·565‡
$(S_{xx} - S_{yy})$	0·02 ± 0·02	0·03 ± 0·02
S_{xy}	0·007 ± 0·007	0·008 ± 0·008
	ϕ_m/(degrees)	
	28·9 ± 0·5	28·9 ± 0·5

† From an iterative fit to the coupling constants of table 4. For an explanation of the two cases, see text.

‡ Fixed at assumed value.

§ For coordinate system 2 of figure 9.

rms errors of both fits are 6 Hz. In case *A*, the inter-ring *z*-axis separation of protons 2 and 6 was held fixed at 1·818 Å corresponding to a C–C inter-ring bridge length of 1·500 Å, $r_{CH} = 1{\cdot}082$ Å, $r_{CC} = 1{\cdot}004$ Å, and a C–C–H angle of 120°. The resulting distortions implied by the r_{ij} of table 7 are quite severe and the order parameters no longer agree with those of Emsley *et al.* [4]. For case *B*, the principal order parameter S_{zz} was held fixed at its value determined in the D_4 symmetry model (table 3). Although several of the internuclear distances are reasonably close to those of table 3, distortions implied by the values for r_{14}, r_{23}, r_{58} and r_{67} still seem unreasonable. For both cases *A* and *B*, the order parameter $S_{xx} - S_{yy}$ is smaller than for the D_4 determination and the same value for ϕ_m, 28·9°, is obtained.

6.4. *Analysis of D_4 couplings from decoupled MQ spectra*

Finally, an analysis of the couplings derived from the decoupled MQ spectrum (table 5) was made with r_{14} held fixed at 4·299 Å. This fit, results of which are given in table 8, exhibited the closest match between calculated and observed couplings (rms deviation only 3 Hz). The value of r_{260} is more in line with the expected value of 1·8 Å but distortions of the rings implied by the other distances are too large to be physically reasonable. The results in table 5 and 8 agree most closely with Emsley *et al.* [4] for their results at 31·5°C, higher than the nominal sample temperature of 28·9°C. This may be a further indication of sample heating caused by the long deuterium decoupling pulse.

Table 8. Internuclear distances, order parameters and dihedral angle for 5CB-d_{11} determined from the coupling constants for the deuterium decoupled multiple-quantum spectrum.†

r_{ij}/(Å)		$S_{\alpha\beta}$§	
r_{12}	2·36 ± 0·03	S_{zz}	0·43 ± 0·01
r_{14}	4·299‡	$(S_{xx} - S_{yy})$	0·06 ± 0·02
r_{23}	4·00 ± 0·10		
r_{260}	1·82 ± 0·05		
	ϕ_m/(degrees)		
	31·6 ± 0·2		

† From an iterative fit to the coupling constants of table 5 and assuming D_4 symmetry.
‡ Fixed at assumed value.
§ For coordinate system 1 of figure 9.

7. Discussion and conclusions

7.1. *Comparison of D_4 and D_2 biphenyl symmetry models*

Overall, the D_4 symmetry model for the biphenyl protons of 5CB-d_{11} produces the most physically reasonable structural parameters from the MQ spectra. The order parameters determined with this model are in closest agreement with those determined by Emsley *et al.* for 5CB-d_{15} protons. The largest difference between the results of these studies exists in the values determined for D_{12}. Our value for this dipolar coupling from the D_4 symmetry

analysis (−4478 Hz) is significantly larger than that reported by Emsley *et al.* (−4220 Hz) at the same temperature [6]. Their experiments involved the protons of only one ring with no dipolar couplings to the alkyl substituted ring. In our D_4 model, we derived a single coupling constant which is taken to be representative of all the ortho couplings of the biphenyl unit. In this sense, the two determinations of D_{12} are not entirely equivalent.

The D_2 analysis presented above deserves closer examination. The values of D_{14} and D_{23} are considerably different and this leads to physically unreasonable internuclear separations. It may be that the spectrum is dependent on the average of these couplings rather than their individual values, as the ratio D_{14}/D_{23} depends only on r_{14}/r_{23}. Indeed, the average of D_{14} and D_{23} in table 4 is close to D_{14} in table 3. This is also true for D_{58} and D_{67}; only their average may be reflected in the spectrum. If this is so, then only 10 coupling values are available to determine the 13 structure/orientation parameters. If the problem is indeed underdetermined in this manner, then ignoring S_{xz} and S_{yz} may not be a valid assumption. A different approach might be to set $r_{14}=r_{23}=r_{58}=r_{67}$. The problem then becomes a determination of 10 parameters (r_{12}, r_{56}, r_{14}, r_{260}, ϕ_m and five $S_{\alpha\beta}$) from the 10 couplings. In light of the successful D_4 analysis, however, we have not yet performed such a calculation. The variance–covariance matrix from the D_2 spectral fit was examined for an indication that the parameters $D_{14}+D_{23}$ and $D_{58}+D_{67}$ are more appropriate than individual values for these couplings. Although significant off-diagonal elements do exist and the pairs D_{14}, D_{23} and D_{58}, D_{67} are certainly correlated, no clear indication was found that the spectrum is only sensitive to the sums $D_{14}+D_{23}$ and $D_{58}+D_{67}$. This does not, however, rule out this possibility. If the couplings are consistent with $r_{14}=r_{23}=r_{58}=r_{67}$, then certain other pairs of couplings (D_{12}, D_{56} and D_{16}, D_{25}) are also probably correlated. It is possible to see that equivalent ring geometries for 5CB-d_{11} might lead to a severely under-determined problem in which all five order parameters cannot be determined simultaneously with the structure.

To our knowledge, inter-ring dipolar coupling constants have not been determined for 5CB prior to our MQ results. For all our different models for the analysis of the MQ spectra, the value found for ϕ_m varied by only a few degrees. We can confidently assign a value of 30 ± 2 degrees to the dihedral angle for 5CB-d_{11}. A more precise determination of this parameter would require a rigorous treatment of vibrational motions.

7.2. *The effects of chemical shifts and heteronuclear couplings on MQ spin–echo spectra*

Throughout our analyses we have neglected chemical shifts and heteronuclear couplings. We now consider how these interactions can lead to distortions in spin–echo MQ spectra and whether the extra splittings in the seven-quantum order might be explained by them. The π pulse in the sequence of figure 2 can potentially cause transfer of the coherence between one pair of eigenstates to a coherence between a different pair for the second half of the evolution period. This coherence transfer problem has recently been analysed by several groups [36, 38–41]. We draw on the relevant features of their results in what follows and concentrate on the coherence transfer effects caused by chemical shifts in an oriented spin system.

The signal sampled at the end of the pulse sequence of figure 2 can be calculated by considering the effect of each pulse and delay interval on the initial equilibrium spin density matrix. This signal, as a function of the MQ evolution delay t, is given by (at a point τ seconds after the last $\pi/2$ pulse and neglecting relaxation) [40]

$$S(t) = \sum_{ijkl} Z_{ijkl} \exp(i\Omega_{ijkl}t), \tag{9}$$

where $\Omega_{ijkl} = (\omega_{ij} - \omega_{kl})/2$ and ω_{ij}, ω_{kl} are the angular frequencies corresponding to differences in the eigenstate energies, i.e. $\omega_{ij} = (E_i - E_j)/\hbar$. The intensity coefficient Z_{ijkl} is determined by the spin hamiltonian, the exact form of the preparation and detection periods of the sequence, and the probability for a coherence transfer between the pairs of states i, j and k, l [40]. For purposes of this discussion, the exact form of Z_{ijkl} is not important; given values for the hamiltonian parameters, Z_{ijkl} can be calculated exactly [36, 40]. Equation (9) states that the π pulse can cause a coherence between states i and j evolving during the first half of the delay t to be transferred to a coherence between states k and l. It can be shown that transfer can only occur between MQ coherences within an order, i.e. $\Delta M_{ij} = \Delta M_{kl}$ [15].

Fourier transformation of the signal in equation (9) with respect to the evolution time t yields the spectrum

$$F(\omega) = \sum_{ijkl} Z_{ijkl}\delta(\omega - \Omega_{ijkl}). \tag{10}$$

When relaxation is included, the delta function of equation (10) can be replaced with a characteristic lineshape function. Thus, the spin–echo MQ spectrum will contain lines at frequencies which are one-half the difference between the MQ frequencies in the absence of a π pulse. The extent to which chemical shifts are removed from MQ evolution will depend on the relative sizes of the dipolar and shift hamiltonians [40].

7.3. *Comparison of the seven-quantum spin–echo spectrum to an AB_2 spin system*

The severity of distortions in the MQ spectrum from coherence transfer effects can be estimated by calculating the intensity coefficients in equation (10). Calculating the spin–echo two-quantum spectrum of an AB_2 system requires much less effort than a calculation of the seven-quantum 5CB-d_{11} spectrum and yet has the same general properties as the larger spin system. For a three spin-1/2 AB_2 system, the eigenstates are classified as either symmetric or antisymmetric under exchange of the B spins [42]. In the symmetric representation, the number of states in each Zeeman manifold for the quantum numbers $M = -3/2, -1/2, 1/2, 3/2$ are 1, 2, 2, 1, respectively. There are two antisymmetric states, one each for $M = -1/2$ and $1/2$. Spin states with Zeeman quantum numbers $M = \pm 4$ and $M = \pm 3$ in the A_1 representation of a D_4 symmetry biphenyl (see figure 7) are similar, in a group theoretical sense, to the six symmetric states of the AB_2 spin system. Introducing a chemical shift difference between the ortho and meta protons will not change the point group from D_4 (unless the chemical differences are different for the two rings). Coherences between the $M = \pm 4$ and $M = \mp 3$ A_1 states of figure 7 lead to the seven-quantum lines of the MQ spectrum. Coherence transfers in the seven-quantum order of 5CB-d_{11} will follow the same trends for the two-quantum coherence transfers of an AB_2 system.

Figure 16 shows theoretical two-quantum spectra for an oriented AB_2 system in which the chemical shift difference, δ_{AB}, is chosen small compared to the dipolar couplings. Figure 16 (*a*) was calculated for the pulse sequence of figure 2, but excluding the π pulse. The spectrum of figure 16 (*b*) is obtained when the π pulse is included. For both spectra, intensities are the result of an average of magnitude spectra calculated for 2000 values of the preparation and detection delay, τ, ranging from 0·05 to 100 ms. The chemical shift, which is present in figure 16 (*a*), is completely eliminated by the π pulse in the spectrum of figure 16 (*b*). Transition frequencies in figure 16 (*b*) are essentially identical to those predicted for $\delta_{AB}=0$. Lines are not split by the action of the π pulse. Artifact lines in figure 16 (*b*) arising from coherence transfers among the four transitions of figure 16 (*a*) fall at roughly the mid-point between the intense lines.

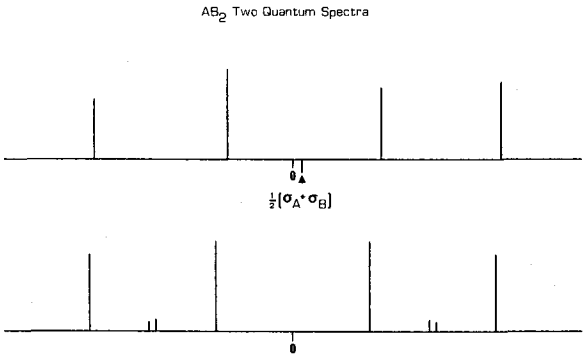

Figure 16. Calculated two-quantum spectra for an anisotropically ordered AB_2 spin-1/2 system. Each spectrum results from the average of 2000 magnitude spectra calculated using different values of the multiple-quantum preparation time τ. (*a*) Predicted spectrum when the π pulse of figure 2 is omitted. The chemical shift difference between A and B spins is not refocused and the spectrum is shifted relative to an arbitrary zero reference. (*b*) When the π pulse is used, the chemical shift is removed and new lines of low intensity arise as a result of coherence transfer effects. Parameters used in the calculations are (in Hz) $D_{AB}=1000$, $D_{BB}=250$, $J_{AB}=10$, $\sigma_A=100$, and $\sigma_B=0$.

Similar calculations were performed for the coupling constants of table 3. Values used for τ fell within the range of those chosen for the experiments. A reasonable range for the chemical shift difference between the ortho and meta protons of 5CB-d_{11} was included in these calculations. The general trend in coherence transfer effects on the seven-quantum spectra was found to be similar to that for the two-quantum AB_2 spectra of figure 16. Line positions in the spin–echo seven- and six-quantum spectral simulations are almost identical to those obtained without a chemical shift difference. Line shifts in the experimental spectra caused by incomplete refocusing of chemical shifts are thus probably smaller than the digital resolution of our spectra. The artifact lines in the calculated spectra are all small and are probably not above the noise level in the experimental spectra. We conclude, therefore, that proton chemical

shift differences in 5CB-d_{11} cannot explain the small splittings in the seven-quantum order not predicted by the D_4 symmetry model. Furthermore, errors introduced by ignoring chemical shifts in the determination of the D_4 coupling constants are probably small.

7.4. *Coherence transfer effects from heteronuclear dipolar couplings*

We have not yet made any computer simulations of the spin–echo spectra to model the effects of heteronuclear dipolar couplings in 5CB-d_{11}. These calculations require a knowledge of the proton–deuterium dipolar coupling constants. For simulated intensities to be accurate, the effects of spin diffusion among the deuterons during the preparation and detection periods would have to be included.

However, coherence transfer effects caused by heteronuclear dipolar couplings in 5CB-d_{11} should be similar to the chemical shift effects described above. Small artifact lines should appear between the intense lines in the seven-quantum spectrum. Our estimate for the largest proton–deuterium dipolar coupling from the decoupling experiments is much smaller than the main seven-quantum splittings in figure 12 (about 4 and 10 kHz). Hence, omitting deuterium decoupling in the experiment may not have lead to any serious distortions of the MQ spin–echo spectrum, and ignoring heteronuclear couplings in the analysis is probably justified.

7.5. *Distortions caused by RF inhomogeneities*

We consider one final explanation for the extra splittings in the spectra: distortions caused by inhomogeneities in the spin–echo refocusing pulse. Such distortions are known to occur in spin–echo spectra of liquid crystals [7, 30]. At this point, inhomogeneous π pulses appear to be the most likely explanation for the lines in the six- and seven-quantum subspectra of figure 4 which evidently do not relate to the proton spin symmetry of 5CB-d_{11}. The effects of RF inhomogeneity can be estimated by simulating spin–echo spectra using some value other than π radians for the rotation propagator of the refocusing pulse. We are currently modifying our computer programs to allow for such a simulation to determine if RF inhomogeneity could have caused the extra splittings.

8. Summary

In this work, we used proton multiple-quantum N.M.R. spectroscopy to determine local order parameters and structure for the biphenyl group of 4-cyano-4′-n-pentyl-d_{11}-biphenyl in its nematic phase. We found that a simple model, in which the phenyl rings are assumed to be equivalent, resulted in the most physically reasonable molecular parameters for 5CB-d_{11}. However, several splittings in the high order MQ spectra were noticed that are inconsistent with this model. A lower symmetry model, in which the phenyl rings were allowed to be inequivalent, is more consistent with the number of experimentally observed lines, but the spectra cannot be used to distinguish between the two symmetries. Molecular parameters determined with the lower symmetry model imply ring distortions which are unacceptable.

We have discussed coherence transfer effects in an MQ spin–echo experiment. Chemical shift inequivalencies among the protons of 5CB-d_{11} do not lead to appreciable distortions of the MQ spectrum obtained by ignoring chemical shifts.

Proton–deuterium dipolar couplings probably only cause slight distortions of the spectrum for an experiment without deuterium decoupling. The poor signal-to-noise ratio in the deuterium decoupled MQ spectrum of 5CB-d_{11} precluded an empirical estimate of these distortions. Distortions from RF inhomogeneities have not yet been ruled out and may provide an explanation for extra splittings not predicted by D_4 symmetry.

Our work has benefited greatly from the insights and ideas of D. P. Weitekamp. We have also had many helpful discussions with G. P. Drobny and W. S. Warren. One of us (D.B.Z.) gratefully acknowledges the receipt of a National Science Foundation Graduate Fellowship. We thank M. P. Klein and the Melvin Calvin Laboratory for making available the computer time necessary for our calculations. This work was supported by the Director, Office of Energy Research, Office of Basic Energy Sciences, Materials Sciences Division of the U.S. Department of Energy under Contract Number DE-AC03-76 F00098.

References

[1] Leadbetter, A. J., Richardson, R. M., and Coling, C. N., 1975, *J. Phys., Paris*, **36**, C1-37. Lyndon, J. E., and Coakley, C. J., 1975, *J. Phys., Paris*, **36**, C1-45.
[2] Emsley, J. W., Lindon, J. C., and Luckhurst, G. R., 1975, *Molec. Phys.*, **30**, 1913.
[3] Boden, N., Clark, L. D., Bushby, R. J., Emsley, J. W., Luckhurst, G. R., and Stockley, C. P., 1981, *Molec. Phys.*, **42**, 565.
[4] Emsley, J. W., Luckhurst, G. R., and Stockley, C. P., 1981, *Molec. Phys.*, **44**, 565.
[5] Emsley, J. W., Luckhurst, G. R., Gray, G. W., and Mosley, A., 1978, *Molec. Phys.*, **35**, 1499.
[6] Sinton, S., and Pines, A., 1980, *Chem. Phys. Lett.*, **76**, 263.
[7] Avent, A. G., Emsley, J. W., and Turner, D. L., 1983, *J. magn. Reson.*, **52**, 57.
[8] Reid, C. J., and Evans, M. W., 1980, *Molec. Phys.*, **40**, 1523.
[9] Schad, Hp., and Osman, M. A., 1981, *J. chem. Phys.*, **75**, 880. Wacrenier, J. M., Duron, C., and Lippens, D., 1981, *Molec. Phys.*, **43**, 97.
[10] Saupe, A., 1964, *Z. Naturf.* (*a*), **19**, 161.
[11] Emsley, J. W., and Luckhurst, G. R., 1980, *Molec. Phys.*, **41**, 19.
[12] Burnell, E. E., and DeLange, C. A., 1980, *J. magn. Reson.*, **39**, 461.
[13] Burnell, E. E., and DeLange, C. A., 1980, *Chem. Phys. Lett.*, **76**, 268.
[14] Emsley, J. W., and Lindon, J. C., 1975, *NMR Spectroscopy Using Liquid Crystal Solvents* (Pergamon).
[15] Sinton, S. W., 1981, Ph.D. Thesis, University of California, Berkeley.
[16] Diehl, P., Kellerhals, H., and Lustig, E., 1972, *NMR: Basic Principles and Progress*, Vol. 6, edited by P. Diehl, E. Fluck and R. Kosfeld (Springer-Verlag).
[17] Aue, W., Bartholdi, E., and Ernst, R. R., 1976, *J. chem. Phys.*, **64**, 2229.
[18] Hatanaka, H., Terao, T., and Hashi, T., 1975, *J. phys. Soc. Japan*, **39**, 835. Hatanaka, H., and Hashi, T., 1975, *J. phys. Soc. Japan*, **39**, 1139.
[19] Pines, A., Wemmer, D., Tang, J., and Sinton, S., 1978, *Bull. Am. phys. Soc.*, **21**, 23.
[20] Drobny, G., Pines, A., Sinton, S., Weitekemp, D., and Wemmer, D., 1979, *Faraday Div. chem. Soc. Symp.*, **13**, 49.
[21] Drobny, G., Pines, A., Sinton, S., Warren, W. S., and Weitekemp, D. P., 1981, *Phil. Trans. R. Soc.* A, **299**, 585.
[22] Warren, W., and Pines, A., 1981, *J. Am. chem. Soc.*, **103**, 1613,
[23] Weitekamp, D. P., *Advances in Magnetic Resonance*, Vol. 11, edited by J. S. Waugh (Academic), pp. 111–274.
[24] Bodenhausen, G., 1981, *Prog. NMR Spectrosc.*, **14**, 137.
[25] Gray, G. W., and Mosley, A., 1976, *Molec. Crystals liq. Crystals*, **35**, 71.
[26] Garbow, J. R., 1983, Ph.D. Thesis, University of California, Berkeley.

[27] PINES, A., VEGA, S., and MEHRING, M., 1978, *Phys. Rev.* B, **18,** 112.
[28] WEITEKAMP, D. P., GARBOW, J. R., and PINES, A., 1982, *J. magn. Reson.*, **46,** 529.
[29] BODENHAUSEN, G., VOLD, R. L., and VOLD, R. R., 1980, *J. magn. Reson.*, **37,** 93.
[30] EMSLEY, J. W., and TURNER, D. L., 1981, *J. chem. Soc. Faraday II*, **77,** 1493.
[31] NIEDERBERGER, W., DIEHL, P., and LUNAZZI, L., 1973, *Molec. Phys.*, **26,** 571.
[32] FIELD, L. D., STERNHELL, S., and TRACEY, A. S., 1977, *J. Am. chem. Soc.*, **99,** 5249. FIELD, L. D., and STERNHELL, S., 1981, *J. Am. chem. Soc.*, **103,** 738.
[33] D'ANNIBALE, A., LUNAZZI, L., BOICELLI, A. C., and MACCIANTELLI, D., 1973, *J. chem. Soc. Perkins II*, 1396.
[34] JONES, R. G., 1969, *NMR : Basic Principles and Progress*, Vol. 1, edited by P. Diehl, E. Fluck and R. Kosfeld (Springer-Verlag), pp. 97–174.
[35] BOTHNER-BY, A. A., and CASTELLANO, S. M., 1968, *Computer Programs for Chemistry* Vol. 1, edited by D. F. Detar (Benjamin).
[36] MURDOCH, J. B., 1982, Ph.D. Thesis, University of California, Berkeley.
[37] DIEHL, P., HENRICHS, P. M., and NIEDERBERGER, W., 1971, *Molec. Phys.*, **20,** 139.
[38] KUMAR, A., 1978, *J. magn. Reson.*, **30,** 227.
[39] KUMAR, A., and KHETRAPAL, C. L., 1978, *J. magn. Reson.*, **30,** 137. KHETRAPAL, C. L., KUMAR, A., KUNWAR, A. C., MATHIAS, P. C., and RAMANATHAN, K. V., 1980, *J. magn. Reson.*, **37,** 349.
[40] TURNER, D. L., 1982, *J. magn. Reson.*, **46,** 213.
[41] THOMAS, M. A., and KUMAR, A., 1982, *J. magn. Reson.*, **47,** 535.
[42] EMSLEY, J. W., FEENEY, J., and SUTCLIFFE, L. H., 1965, *High Resolution NMR Spectroscopy*, Vol. 1 (Pergamon), Chap. 8.